Available online at www.sciencedirect.com
ScienceDirect
Lithos 93 (2007) 199–213
LITHOS
www.elsevier.com/locate/lithos

Diamonds from the Buffalo Head Hills, Alberta: Formation in a non-conventional setting

Anetta Banas [a,*], Thomas Stachel [a], Karlis Muehlenbachs [a], Tom E. McCandless [b]

[a] *Department of Earth and Atmospheric Sciences, 1-26 Earth Sciences Building, University of Alberta, Edmonton, Alberta, Canada T6G 2E3*
[b] *Ashton Mining of Canada Inc. Unit 116-980 West 1st Street, North Vancouver, B.C. Canada V7P 3N4*

Received 13 June 2005; accepted 3 July 2006
Available online 7 August 2006

Abstract

Kimberlite pipes K11, K91 and K252 in the Buffalo Head Hills, northern Alberta show an unusually large abundance (20%) of Type II (no detectable nitrogen) diamonds. Type I diamonds range in nitrogen content from 6 ppm to 3300 ppm and in aggregation states from low (IaA) to complete (IaB). The Type IaB diamonds extend to the lowest nitrogen concentrations yet observed at such high aggregation states, implying that mantle residence occurred at temperatures well above normal lithospheric conditions. Syngenetic mineral inclusions indicate lherzolitic, harzburgitic, wehrlitic and eclogitic sources. Pyropic garnet and forsteritic olivine characterize the peridotitic paragenesis from these pipes. One lherzolitic garnet inclusion has a moderately majoritic composition indicating a formation depth of ~ 400 km. A wehrlitic paragenesis is documented by a Ca-rich, high-chromium garnet and very CaO-rich (0.11–0.14 wt.%) olivine. Omphacitic pyroxene and almandine-rich garnet are characteristic of the eclogitic paragenesis. A bimodal $\delta^{13}C$ distribution with peaks at −5‰ and −17‰ is observed for diamonds from all three kimberlite pipes. A large proportion (~ 40%) of isotopically light diamonds ($\delta^{13}C < -10‰$) indicates a predominantly eclogitic paragenesis.

The Buffalo Head Terrane is of Lower Proterozoic metamorphic age (2.3–2.0 Ga) and hence an unconventional setting for diamond exploration. Buffalo Hills diamonds formed during multiple events in an atypical mantle setting. The presence of majorite and abundance of Type II and Type IaB diamonds suggests formation under sublithospheric conditions, possibly in a subducting slab and resulting megalith. Type IaA to IaAB diamonds indicate formation and storage under lower temperature in normal lithospheric conditions.

Keywords: Diamond inclusions; Carbon isotopes; Nitrogen aggregation; Majorite; Off-craton

1. Introduction

Traditionally diamond exploration has focused on cratons stabilized in the Archean with no subsequent tectonothermal activity. This approach is based on an empirically derived association of primary diamond deposits with Archean cratons as summarized by Janse (1994). Exploration in an unconventional (post-Archean) geological setting resulted in the discovery of the Buffalo Hills kimberlite field in northern Alberta. It was discovered in 1997 by re-examination of aeromagnetic and geophysical surveys, and explored by the Ashton/Encana/Pure Gold joint venture. The subcontinental lithospheric mantle beneath the Buffalo Head Terrane has been characterized using xenocryst and xenolith compositions in studies conducted by Aulbach et al. (2004) and Hood and McCandless (2004). Aulbach

* Corresponding author. Fax: +1 780 492 2030.
E-mail address: abanas@ualberta.net (A. Banas).

0024-4937/$ - see front matter © 2006 Elsevier B.V. All rights reserved.
doi:10.1016/j.lithos.2006.07.001

et al. (2004) reported a subcontinental lithospheric mantle composition dominated by lherzolite with minor components of wehrlite, websterite, pyroxenite and eclogite; and define a geotherm of 38–39 mW/m^2 from garnet xenocryst compositions. Hood and McCandless (2004) identified predominantly high-Cr lherzolitic garnets with only a very small proportion of harzburgitic garnets present. The almost complete absence of subcalcic garnets indicates a post-Archean signature (Griffin et al., 1999), unambiguous evidence of Archean precursors probably having been eliminated by subsequent tectonothermal and metasomatic events (Aulbach et al., 2004). Additional information about the composition of the lithospheric mantle is derived from the analysis of diamonds and their syngenetic inclusions. Diamonds from the K10 and K14 kimberlite diatremes were examined by Davies et al. (2004). They recovered inclusions in diamonds which agree with the compositions found in the xenolith and xenocryst populations. Davies et al. (2004) proposed that diamond formation beneath the Buffalo Head Terrane occurred in a dynamic mantle environment such as a plume.

Subsequent discoveries of diamondiferous kimberlites, such as K252 with a diamond grade of 55 cts/100 tonnes, have rejuvenated interest in the region and facilitated further study into this atypical setting. Diamonds from three additional kimberlite pipes, K11, K91 and K252, were examined and classified according to morphology, carbon isotope composition, nitrogen content and aggregation state, and mineral inclusion chemistry. The results provide further constraints and new insights into the formation of diamonds and composition of the subcontinental mantle beneath the Buffalo Head Terrane.

2. Geological setting

The Buffalo Hills kimberlite field consists of 38 kimberlite pipes, 26 of which are diamondiferous (Hood and McCandless, 2004). The field is located in north–central Alberta and lies within the confines of the Buffalo Head Terrane (Fig. 1). The Buffalo Head Terrane is of Lower Proterozoic metamorphic age (2.3–2.0 Ga) with presumed Archean precursors (Theriault and Ross, 1991; Villeneuve et al., 1993). It is bounded to the north by the Great Slave Lake shear zone, and bordered by the Taltson, Wabamun and Chinchaga domains to the east, south and west, respectively. The basement rocks are overlain by up to 1600 m of Devonian and Cretaceous sedimentary deposits (Mossop and Shetsen, 1994). The area is variably covered by Quaternary till, glaciofluvial and glaciolacustrine deposits which in places exceed 100 m in thickness (Carlson et al., 1999). The Buffalo Hills kimberlite diatremes intrude into the sedimentary bedrock, and are seismically imaged to reach below the Phanerozoic–Proterozoic boundary (Carlson et al., 1999). Drilling is restricted to the uppermost 200 m, but from seismic it can be inferred that most bodies are steep-sided, carrot shaped pipes that contain crater facies lithologies (Carlson et al., 1999). The pipes range in size from less than 1 to 47 ha with U–Pb perovskite emplacement ages between 88 and 85 Ma (Carlson et al., 1999; Eccles et al., 2003).

3. Samples and techniques

3.1. Samples

All diamonds (~ 700) recovered from pipes K11, K91 and K252 were examined and classified according to morphology and color. The diamonds were recovered through hand picking of heavy mineral concentrate. A set of 107 diamonds, 0.4–3.3 mm in size, was selected for FTIR (Fourier Transform Infrared) analyses to quantify nitrogen concentrations and characterize nitrogen defects. A subset of twenty-two diamonds, 0.6–1.2 mm in size, was further analyzed for their carbon isotope composition. A second set of 54 diamonds (<1.2 mm) was chosen for complete analyses including nitrogen, carbon and mineral inclusion analyses.

3.2. Analytical techniques

Analytical studies included the characterization of diamond morphology, surface features and color, infrared spectroscopy, carbon isotopic analyses and identification, extraction and analysis of mineral inclusions.

Nitrogen concentrations and aggregation states were determined using a Thermo-Nicolet Fourier Transform Infrared (FTIR) spectrometer coupled with a Continuum microscope equipped with a KBr beam splitter. The system was purged with a dry nitrogen–oxygen mix to maintain a stable environment. Analyses were carried out on fragments from crushed diamonds (samples A100-141, A200-208, A300-303) and on whole diamonds (samples B100-174, B200-211, B300-318). Spectra (600–4000 cm^{-1}) were collected for 200 s with a spectral resolution of 4 cm^{-1} and an aperture ranging between 50 and 100 μm (determined by sample size). A Type II diamond standard was measured and, after baseline correction, converted to absorption coefficient through normalization of the absorbance at 1995 cm^{-1} to 11.94 cm^{-1}. Sample spectra were first baselined and then the normalized Type II spectrum was

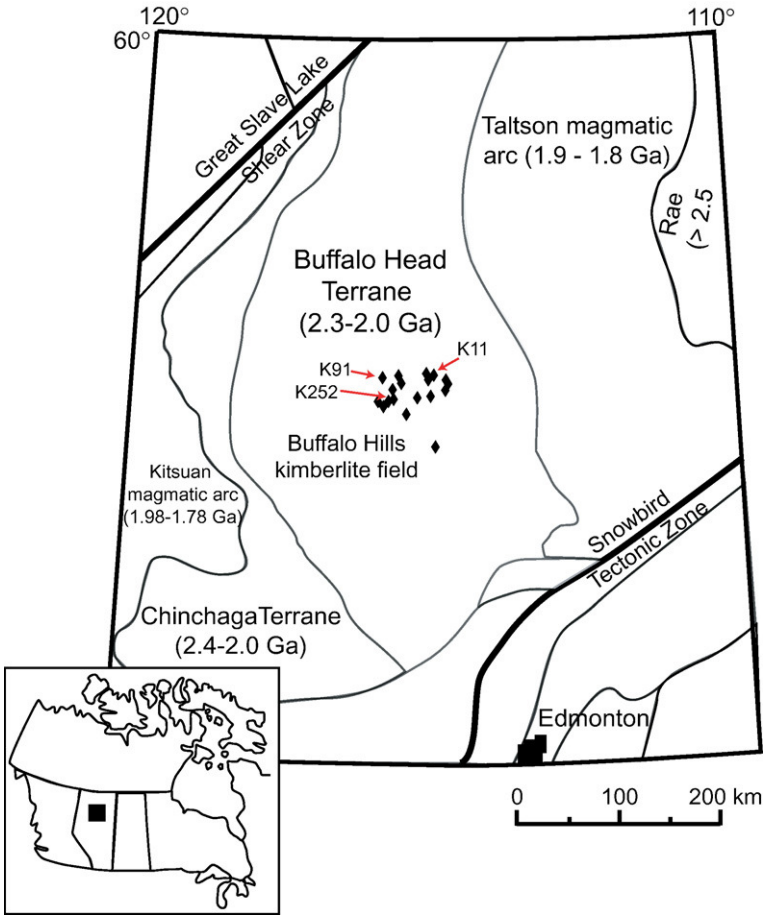

Fig. 1. Locality map of the Buffalo Head Terrane (after Eccles et al., 2003).

"subtracted": a process involving normalization of the sample diamond spectrum to the Type II reference spectrum. This subtraction removes the two phonon (pure diamond) absorption and converts the spectrum to absorption coefficient simultaneously. Spectral deconvolution was used to determine nitrogen contents and aggregation states, based on software provided by David Fisher (Research Laboratories of the Diamond Trading Company, Maidenhead, UK). Nitrogen concentrations (atomic ppm) were calculated from absorption coefficient values at 1282 cm^{-1} using the factors derived by Boyd et al. (1994a) for the A-center and Boyd et al. (1995) for the B-center. Detection limits and errors are strongly dependant on sample quality but typically range from 5 to 15 ppm and about 5–10% of the concentration respectively.

Carbon isotope ratios were measured with a Finnigan Mat 252 Mass Spectrometer, with a precision of ±0.1‰. Diamond fragments (0.5–1.5 mg) were combusted (at 980 °C) for 10 h in evacuated silica glass tubes with 1.0–2.0 g of CuO to ensure oxidation. Carbon isotope ratios are reported relative to the VPDB standard.

Mineral inclusions were extracted from the diamonds using a steel crusher. Syngenetic mineral inclusions were identified as primary prior to breakage by the absence of fractures around the inclusion connected to the diamond surface and their geometric shapes. Epigenetic inclusions were identified by the presence of fractures reaching from the inclusion to the diamond surface and their altered appearance once released from the diamond. The recovered inclusions were placed in brass pips, set in Araldite epoxy and polished. Major element concentrations were measured using a JEOL 8900 Electron Microprobe with an accelerating voltage of 15 keV and a beam current of 20 nA. Peak count times were 15–20 s and background time was half the peak time. Three spots were measured on each sample and averaged. Resulting detection limits are ~ 0.03 wt.%.

A reference database (Stachel and Harris, 1997a; Stachel et al., 2000) is used to compare the mineral

Table 1
Physical, carbon isotope and nitrogen characteristics and inclusions in diamonds from the Buffalo Heads Hills, Alberta

Pipe	Sample	Weight (mg)	Morphology	Col.	P.D.	$d^{13}C$ (‰)	N (ppm)	%B	Type	H	Para.	Assem.
K252	A100	2.7	agg thh	c	n	−6.40	116	0	IaA	n		serp
K252	A101	1.8	thh	ly	n	−7.71	18	41	IaAB	n		
K252	A102	2.9	thh	b	n	−4.71	0		II	n		serp
K252	A103	1.1	thh	b	n	−4.13	0		II	y		
K252	A104	1.6	twin thh	c	n	−6.73	1494	12	IaAB	y		
K252	A105	1.2	thh	b	y	−5.93	940	17	IaAB	y		
K252	A106	1.8	thh frag	b	y	−20.99	39	97	IaB	y		
K252	A107	1.5	thh	b	y	−18.06	140	97	IaB	y		
K252	A109	2.4	thh	c	y	−16.19	16	71	IaAB	y		calc
K252	A110	1.9	thh	c	n	−17.38	38	0	IaA	y	e	grt
K252	A111	1.7	thh	c	n	−14.80	ns					
K252	A112	3.1	thh	c	n	−15.84	0		II	y	p	ol
K252	A113	1.9	thh	b	n	−17.93	ns					
K252	A114	1.6	thh	c	n	−7.91	738	2	IaA	n		
K252	A115	1.7	thh	b	y	−17.60	14	32	IaAB	y	e	grt
K252	A116	2.4	twin thh	b	n	−15.36	23	100	IaB	y		
K252	A117	2.4	twin thh	c	n	−17.17	75	100	IaB	y		
K252	A118	2.1	thh	c	n	−5.29	0		II	y		
K252	A119	2.8	twin thh	c	n	−15.12	140	100	IaB	y	e	cpx
K252	A120	1.8	thh	lb	y	−6.54	2267	15	IaAB	y		
K252	A121	2.1	agg octa	b	n	−13.90	1359	100	IaB	y		
K252	A122	2.2	thh frag	c	n	−8.40	0		II	y		
K252	A123	0.7	thh frag	c	n	−3.94	0		II	n	e	grt
K252	A124	0.4	agg thh	c	n	−17.24	99	100	IaB	y		
K252	A125	0.8	irr	c	y	−15.30	1615	100	IaB	y		
K252	A126	2.0	octa frag	c	n	−13.95	0		II	y		
K252	A127	0.5	thh frag	y	n	−4.74	24	100	IaB	y		serp
K252	A128	2.6	thh frag	c	y	−6.84	37	100	IaB	y	e	grt
K252	A129	1.4	thh frag	c	y	−10.19	0		II	y		
K252	A130	2.6	thh frag	c	n	−8.00	131	100	IaB	y		serp
K252	A131	1.8	irr	b	y	−7.69	913	1	IaA	y	e	cpx
K252	A132	2.6	thh	c	y	−4.67	505	10	IaA	n		
K252	A133	3.1	thh	b	n	−17.30	18	91	IaB	y		serp
K252	A134	2.3	thh frag	c	n	−8.53	1571	16	IaAB	y		
K252	A135	4.6	agg thh	b	y	−13.27	23	100	IaB	y		serp
K252	A136	2.3	agg thh	lb	y	−15.52	1242	98	IaB	y		
K252	A137	2.4	agg thh	c	n	−5.59	34	50	IaAB	y		
K252	A138	2.3	thh	c	n	−3.10	0		II	n		
K252	A139	1.5	agg thh	b	n	−15.52	0		II	y		
K252	A140	3.0	agg thh	b	y	−13.75	95	100	IaB	n		
K252	A141	1.5	thh frag	c	n	−22.78	88	53	IaAB	y	wh	grt
K252	B103	0.8	thh frag	c	y	−5.77	0		II	n		
K252	B110	1.7	octa frag	c	n	−2.48	0		II	y		
K252	B111	0.9	agg octa	b	n	−6.39	91	24	IaAB	n		
K252	B122	2.9	thh	c	n	−3.26	1842	0	IaA	y		
K252	B127	1.4	frag	ly	n	−10.37	607	72	IaAB	y		
K252	B138	0.4	agg octa	c	n	−6.37	374	14	IaAB	y		
K252	B143	0.5	thh	c	n	−4.67	1819	44	IaAB	y		
K252	B152	1.1	octa frag	c	n	−2.77	15	97	IaB	y		
K252	B153	1.0	thh	c	n	−6.13	1474	9	IaA	y		
K252	B157	1.3	frag	c	y	−3.85	108	76	IaAB	y		
K252	B171	0.3	twin octa	c	n	−3.01	132	89	IaAB	y		
K11	A201	2.9	octa frag	c	n	−3.65	0		II	n	e	
K11	A202	0.9	agg octa	c	n	−7.81	0		II	n		
K11	A203	3.1	irr	c	n	−3.59	17	27	IaAB	n		
K11	A204	2.6	irr	c	n	−8.61	0		II	n		
K11	A205	1.0	thh frag	c	n	−11.03	6	92	IaB	y	p	
K11	A206	0.1	octa	y	n	−6.07	0		II	y	p	

Table 1 (*continued*)

Pipe	Sample	Weight (mg)	Morphology	Col.	P.D.	$d^{13}C$ (‰)	N (ppm)	%B	Type	H	Para.	Assem.
K11	A207	1.8	thh	c	n	−4.33	0		II	n		
K11	A208	1.5	irr	c	n	−16.62	0		II	n		
K11	A209	2.2	agg octa	ly	n	−5.61	0		II	y	p	
K11	B201	0.2	twin octa	lb	n	−5.86	9	0	IaA	n		
K11	B202	1.5	twin thh frag	lb	n	−6.52	0		II	n		
K11	B204	0.3	frag	y	n	−16.93	45	51	IaAB	y		
K11	B208	0.5	octa frag	c	n	−5.70	15	21	IaAB	y		
K91	A301	2.9	twin thh	c	n	−5.83	1005	23	IaAB	n		
K91	A302	1.7	thh frag	y	n	−13.57	62	40	IaAB	y		
K91	A303	1.2	octa	c	y	−17.98	292	100	IaB	y		
K91	A304	2.0	octa	c	n	−4.26	232	100	IaB	y		
K91	B301	0.5	frag	b	n	−9.61	38	98	IaB	y		
K91	B302	1.4	frag	c	n	−8.87	860	37	IaAB	y		
K91	B303	1.6	frag	c	n	−19.51	2080	65	IaAB	y		
K91	B311	2.3	thh	c	n	−5.10	2263	5	IaA	y		
K91	B317	0.4	octa	c	n	−3.03	735	100	IaB	y		
K91	B318	1.8	thh	c	n	−4.01	3280	100	IaB	y		

thh=tetrahexahedroida, frag=fragment, octa=octahedra, irr=irregular, agg=aggregate, part res=partially resorbed; Col.=color: c=colorless, b=brown, lb=light brown, y=yellow, ly=light yellow, lg=light grey; P.D.=plastic deformation, H=hydrogen, Para.=paragenesis: p=peridotitic, e=eclogitic, wh=wehrlitic; Assem.=mineral assemblage: grt=garnet, cpx=clinopyroxene, ol=olivine, serp=serpentine, calc=calcite, biot=biotite, dol=dolomite, calc=calcite; ns=no suitable samples.

inclusion chemistry, the carbon isotopic compositions, and the nitrogen contents and aggregation states of the host diamonds to those from worldwide sources.

4. Diamond characteristics

4.1. Color

The diamonds show a range of colors from colorless to yellow and brown, and overall are mainly transparent (Table 1 and Supplementary Table 1). Colorless diamonds are most abundant, comprising ~ 60% of the population of each pipe. Brown colors range from light to dark, and are often associated with evidence of plastic deformation (c.f. Harris, 1992). There are no significant differences between the color distributions for each pipe.

4.2. Morphology

Diamond morphologies include octahedral, tetrahexahedroidal, cuboid as well as twinned and aggregated forms (Table 1 and Supplementary Table 1). Diamond fragments are categorized according to their residual primary features. Irregular shaped stones show no recognizable features and are grouped separately.

The majority of crystals, ~ 45%, exhibit tetrahexahedroidal morphologies resulting from resorption of octahedra. The term tetrahexahedroidal is used in this study to describe resorbed diamond morphologies according to the scheme proposed by Robinson (1979), commonly, in the literature, these shapes are referred to as dodecahedral. There are no major differences in morphological distribution between different size classes or pipes (Fig. 2). Twins are most common in K252 but are present in smaller quantities in the other two pipes. Octahedral/tetrahexahedroidal ratios for twins and aggregates are similar to those for single crystals. Cubes are found only in K252, but form only a very minor component.

4.2.1. Octahedra

Sharp edged octahedra with smooth faces dominate the octahedral population (Fig. 3a). About 0.5% of diamonds show pronounced development of triangular plates (a growth feature) and may be classified as stacked octahedra. Other octahedral surface textures, evident on a minority of the population, are dominated by resorption and etch features: ~ 10% of octahedra show minor shield laminae and serrate laminae (Fig. 3b). Negative trigons are abundant on approximately 30% of the crystal faces (Fig. 3b) and hexagons were noted on 2% of crystal faces. A small proportion of octahedra show signs of minor resorption along the crystal edges tending toward tetrahexahedroidal shapes; crystals with less than 10% resorbed features were classified as octahedra.

4.2.2. Tetrahexahedroida

Tetrahexahedroidal crystals form through the resorption of octahedra (Robinson et al., 1989; Fig. 3c). Varying stages of resorption from partial to complete are

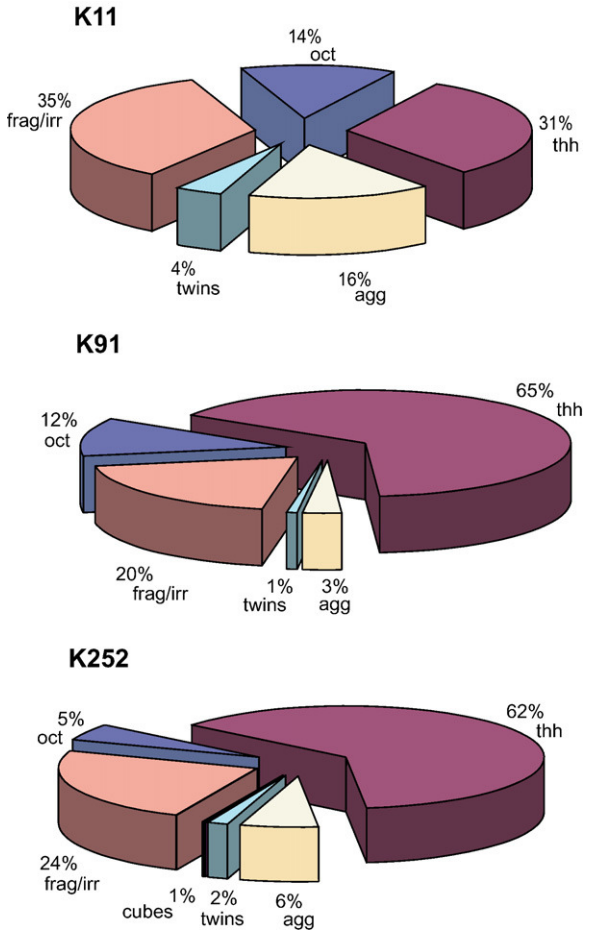

Fig. 2. Distribution of diamond shapes between pipes K11, K91 and K252. The tetrahexahedroidal shape dominates the distribution in all 3 pipes. Octahedral/tetrahexahedroidal ratios for twins and aggregates are not distinct from single crystals. Abbreviations are the same as used in Table 1.

observed; incomplete resorption with residual octahedral faces is quite common. Tetrahexahedroidal faces are invariably covered with hillock patterns. Three types of hillock patterns were distinguished: 1) fine, narrow, elongate hillocks (Fig. 3d), 2) flat, broad hillocks, 3) pyramidal, high relief hillocks. The majority of crystal faces have rough, dull textures usually associated with an abundance of fine hillocks. This often makes the interior of the diamonds difficult to examine. A minority of tetrahexahedroida has smooth, shiny faces associated with the latter two types of hillock patterns (Fig. 3c).

4.2.3. Twins

Twinned crystals are represented by contact (macles) and interpenetrant twins with octahedral and tetrahexahedroidal morphologies (Fig. 3e). Twins are readily recognized by the presence of twin planes, often expressed by a herringbone pattern in the case of macles. In many tetrahexahedroidal samples it is difficult to identify the twin plane due to extensive resorption but a flattened crystal shape may indicate the presence of twinning. Surface features of twinned crystals are the same as those observed on single crystals.

4.2.4. Aggregates

A small proportion of aggregated crystals with octahedral and tetrahexahedroidal morphology is present. The aggregates observed are formed from 3 up to 6 crystals. The surface features are the same as those observed on single crystals.

4.2.5. Irregular

Irregular crystals have no defining characteristics that allow them to be classified into the above groups. They are commonly fragments with breakage surfaces (both fresh and resorbed) on all sides and no remnant recognizable faces.

4.3. Deformation

Deformation, recognized by the presence of lamination lines, was observed in 17% of the diamonds. Lamination lines occur as single or multiple sets of fine lines, parallel to {111}. Lamination lines along all four octahedral planes have previously been observed on individual stones (Harris, 1987), however, usually only one or less commonly up to two sets were observed from this locality (Fig. 3f). An additional indicator of deformation may be color; Orlov (1973) relates brown coloration to plastic deformation. If lamination lines and color are taken into account ~ 35% of diamonds indicate some form of plastic deformation. Identification of plastically deformed crystals becomes important when considering the effects of nitrogen aggregation as discussed below.

5. Mineral inclusions in diamond

Mineral inclusions of the eclogitic and peridotitic suites, ranging in size from 15–60 μm, were recovered from a restricted sample set. Fourteen of the twenty-seven inclusions were determined to be epigenetic. Table 1 lists the inclusion abundance and distribution among the pipes, electron microprobe analyses are reported in Table 2.

5.1. Syngenetic inclusions

5.1.1. Garnet

Five garnet inclusions were recovered from four diamonds. Garnet inclusion parageneses can be identified

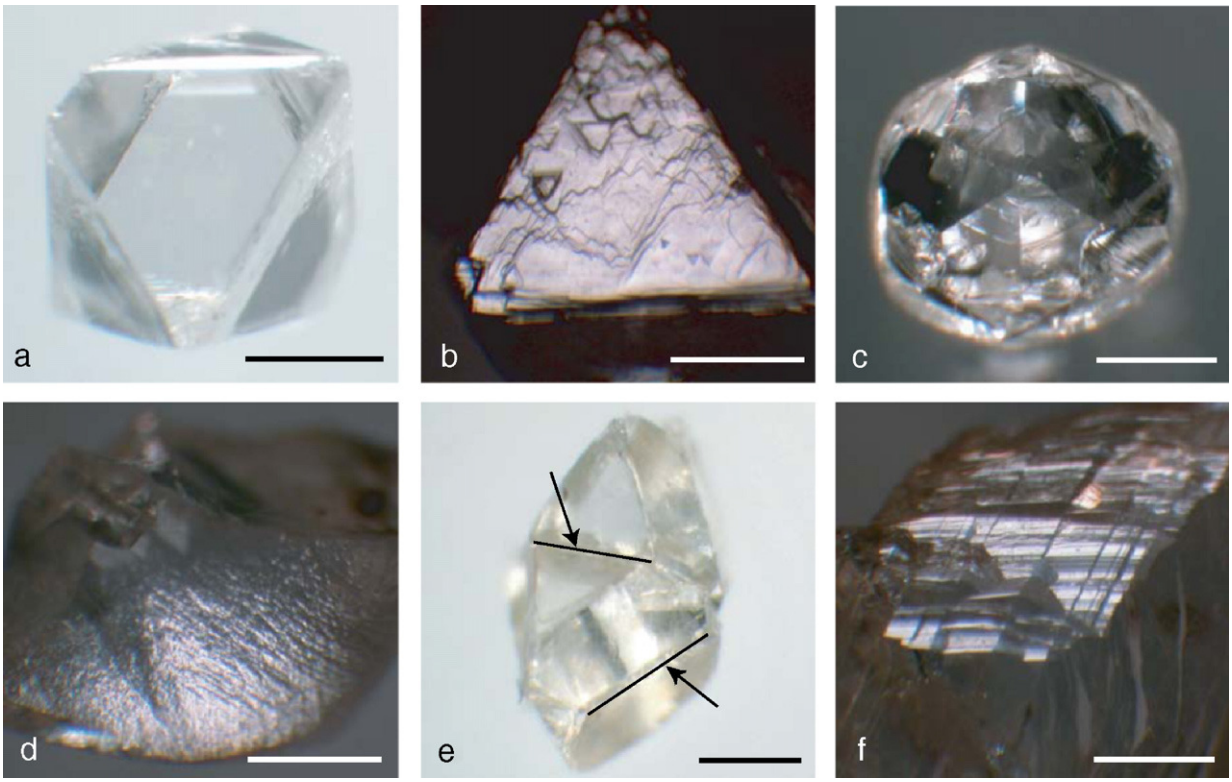

Fig. 3. Characteristic features of diamonds from K11, K91, K252: a) Sharp-edged octahedron, colorless and transparent. b) Octahedral face with minor negative trigons and abundant serrate laminae. c) Fully resorbed colorless tetrahexahedroid. Shows smooth, shiny face with broad, flat hillocks (pattern 2 and 3, see text). d) Fine, narrow elongate hillocks (pattern 1, see text) on tetrahexahedroidal face, produce rough surface texture and dull appearance. e) Doubly twinned octahedral crystal, twin planes are indicated by arrows. f) Brown colored tetrahexahedroidal fragment showing lamination lines (evidence of plastic deformation). Scale bars represent 500 μm.

by their CaO and Cr_2O_3 content (Gurney et al., 1984; Sobolev et al., 1973). Three garnet inclusions plot within the eclogitic field with Cr_2O_3 contents less than 2 wt.% and CaO contents that fall within the normal range for eclogitic garnet inclusions worldwide (Fig. 4). Davies et al. (2004) reported nine eclogitic garnets from pipe K14 with compositions that are consistent with our findings but extend the compositional range to higher CaO contents.

Table 2
Electron microprobe analyses of mineral inclusions in Buffalo Head Hills diamonds

Sample	A115-1	A115-2	A128	A141	A209	A112	A205-1	A205-2	A206	A119-1	A119-2	A131	A201
Mineral	grt	grt	grt	grt	maj-grt	ol	ol	ol	ol	cpx	cpx	cpx	rutile
Paragenesis	E	E	E	Wh	P	P	P	P	P	E	E	E	E
SiO_2	39.6	39.9	38.9	40.7	43.9	40.2	39.3	40.8	40.5	55.1	53.4	50.0	≤0.03
TiO_2	0.94	0.95	0.95	0.45	0.10	≤0.03	≤0.03	≤0.03	≤0.03	0.22	0.23	0.94	99.02
Al_2O_3	21.5	21.6	21.8	18.8	13.0	≤0.03	≤0.03	≤0.03	≤0.03	7.35	7.71	2.03	0.39
Cr_2O_3	0.12	0.11	0.11	5.37	6.32	≤0.03	≤0.03	≤0.03	≤0.03	≤0.03	≤0.03	≤0.03	≤0.03
MgO	10.8	10.5	10.1	18.2	22.0	49.8	50.8	48.9	50.6	10.4	10.1	14.7	≤0.03
CaO	7.48	7.50	7.93	7.06	5.34	≤0.03	0.11	0.14	0.03	15.0	16.9	19.0	≤0.03
MnO	0.48	0.49	0.49	0.36	0.29	0.15	0.10	0.11	0.09	0.06	0.06	0.36	≤0.03
FeO	19.6	19.6	20.5	8.11	8.43	9.59	8.80	8.88	8.04	6.05	6.35	12.2	0.41
Na_2O	0.33	0.34	0.35	0.05	0.24	≤0.03	0.04	≤0.03	0.07	4.29	4.16	0.28	≤0.03
K_2O	≤0.03	≤0.03	≤0.03	≤0.03	≤0.03	≤0.03	≤0.03	≤0.03	≤0.03	≤0.03	0.04	≤0.03	≤0.03
Oxide total	100.96	101.08	101.22	99.15	99.56	100.05	99.28	98.97	99.37	98.53	99.08	99.51	99.90

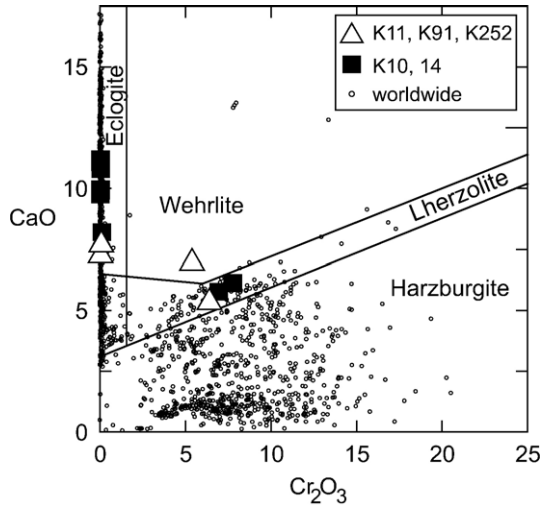

Fig. 4. CaO vs Cr_2O_3 for garnet inclusions in diamond. Open symbols K11, K91, K252: this study; solid symbols K10, K14: Davies et al. (2004). Lherzolite field from Sobolev et al. (1973).

A pyropic garnet inclusion with 6.2 wt.% Cr_2O_3 plots within the lherzolitic field in Fig. 4. Davies et al. (2004) recovered two more lherzolitic garnet inclusions with slightly higher Cr_2O_3 contents. Our lherzolitic garnet has a moderate majorite component recognized by an excess of Si (6.41 Si cations per formula unit based on 24 oxygens; Fig. 5). Based on the experimental data of Irifune (1987) a depth of ~ 400 km is implied for the formation of this garnet. From K14 Davies et al. (2004) report majoritic garnet inclusions of the eclogitic suite with associated depths of formation ranging from ~ 300 to 370 km.

A second peridotitic garnet inclusion, recovered from K252, shows an affinity with the wehrlitic paragenesis. It has a CaO content of 7.2 wt.% and Cr_2O_3 of 5.8 wt.% and thus plots above the lherzolite field in Fig. 4. This paragenesis is rare as an inclusion in diamond, with only three previous occurrences having been reported: Ellendale, (Jaques et al., 1989); Udachnaya, (Sobolev et al., 1984); Yakutia, (Sobolev et al., 2004). However, a wehrlitic paragenesis has been observed from numerous kimberlite occurrences, particularly in Canada (Kopylova et al., 2000), including xenocrysts from the Buffalo Hills (Aulbach et al., 2004; Hood and McCandless, 2004).

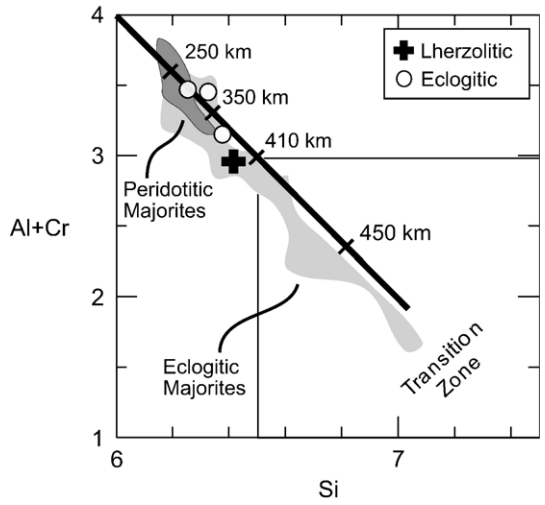

Fig. 5. Atomic proportions of Al+Cr plotted vs. Si (based on 24 oxygen). Majoritic garnets show formation beneath the lithosphere (>250 km). The three eclogitic majorites are from Davies et al. (2004). Depth estimates are based on the experimental data of Irifune (1987) obtained at 1200 °C. Compositional fields of eclogitic and peridotitic majorites from worldwide occurrences are shown for reference.

5.1.2. Olivine

Four olivine inclusions were recovered from three diamonds: one from K252 and three from K11. The olivines have Fo contents between 90.7 and 91.8 mol%. Two olivines from the current study have CaO contents that are too low (below 0.04 wt.%) to have crystallized in equilibrium with clinopyroxene indicating a harzburgitic affinity (Fig. 6). Davies et al. (2004) also recovered two olivines with CaO contents below 0.04 wt.% although with higher Fo contents. Two olivines have CaO contents which are unusually high (0.11 and 0.14 wt.%) indicating that they crystallized in a Ca-rich wehrlitic environment where Ca in olivine is not buffered by the presence of orthopyroxene (Köhler

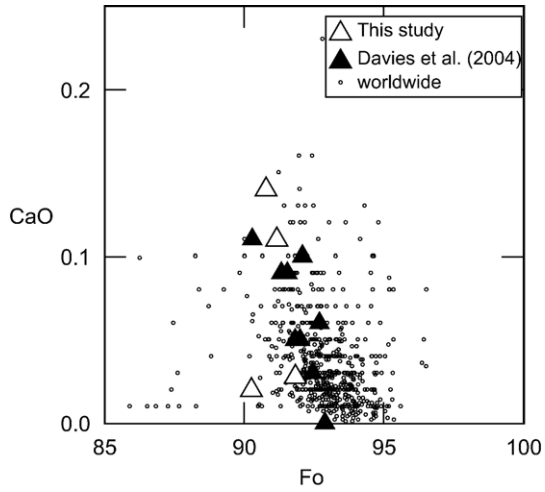

Fig. 6. CaO wt.% vs. Fo (100*Mg/Mg+Fe) content for olivine inclusions. Olivine inclusions with CaO<0.04 wt.% are of harzburgitic paragenesis. Olivine inclusions with CaO 0.11–0.14 wt.% are of wehrlitic affinity.

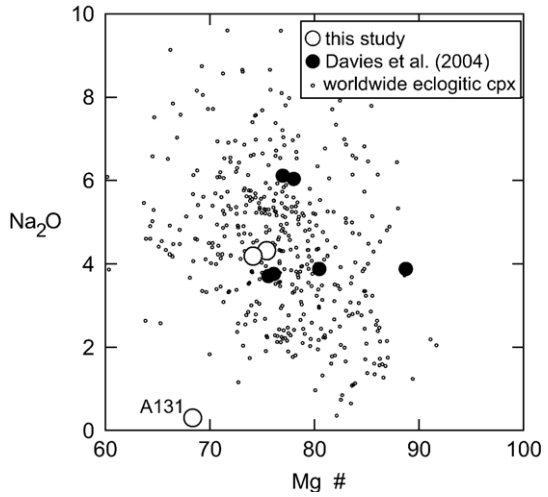

Fig. 7. Clinopyroxene compositions from Buffalo Hills diamonds plot within worldwide database for eclogitic clinopyroxenes, the exception being A131 with the composition of an augite.

and Brey, 1990). Davies et al. (2004) report two olivine inclusions with similarly high CaO contents as well as several olivines with intermediate CaO contents representing lherzolitic and harzburgitic parageneses.

5.1.3. Clinopyroxene

Three clinopyroxene inclusions were recovered from two diamonds from K252. These inclusions have low Cr_2O_3 contents (≤ 0.03 wt.%), Mg # (100*Mg/Mg+Fe) of 67–72 and variable Ca # (100*Ca/Ca+Mg+Fe) of 39–47 (Fig. 7), characteristics that place them within the eclogitic paragenesis. Two inclusions have Na_2O and Al_2O_3 contents indicative of an omphacitic character. The third (A131) inclusion has low Na_2O and Al_2O_3 and may be classified as an augite. Davies et al. (2004) report clinopyroxene inclusion compositions that span the eclogitic (shown in Fig. 7), websteritic and peridotitic parageneses.

5.1.4. Rutile

One rutile inclusion was recovered from diamond A201 from pipe K11. Analyses reveal the presence of trace amounts of FeO and Al_2O_3. Rutile is associated with the eclogitic paragenesis (Meyer, 1987).

5.2. Epigenetic inclusions

Epigenetic inclusions are found as fracture infillings and altered primary phases. Epigenetic inclusions were recovered from all three pipes and included serpentine, calcite, dolomite and biotite and are not further considered.

6. Carbon isotopic composition

A subset of 77 samples, spanning the whole range of nitrogen contents and aggregation states, was selected for carbon isotope analyses. These samples show a range in carbon isotopic composition from −22.8‰ to −2.5‰, with a bimodal distribution and modes around −5‰ and −17‰ (Fig. 8). No correlation between carbon isotopic composition and morphology or color was observed. The lower $\delta^{13}C$ population (mode at −17‰) is dominated by diamonds of eclogitic paragenesis as indicated by the presence of eclogitic inclusions. Two of the samples with peridotitic inclusions also plot within this lower range, one of which contains the wehrlitic garnet and this diamond has the lightest measured composition at −22.8‰. The higher peak at −5‰ is populated by diamonds of both peridotitic and eclogitic paragenesis.

Davies et al. (2004) report isotopic data for 39 samples from pipes K10 and K14. $\delta^{13}C$ values range from −20.6‰ to −2.7‰ and again has a bimodal distribution (modes at −5‰ and −15‰) in agreement with this study.

Worldwide, diamonds have a broad range in carbon isotope composition from −30‰ to +3‰ with a normal distribution (mode ~ −5‰). Peridotitic diamonds are mainly restricted to values between −10 and −2‰ whereas eclogitic diamonds have isotopic compositions that span the whole range (Cartigny et al., 1998a,b; Kirkley et al., 1991).

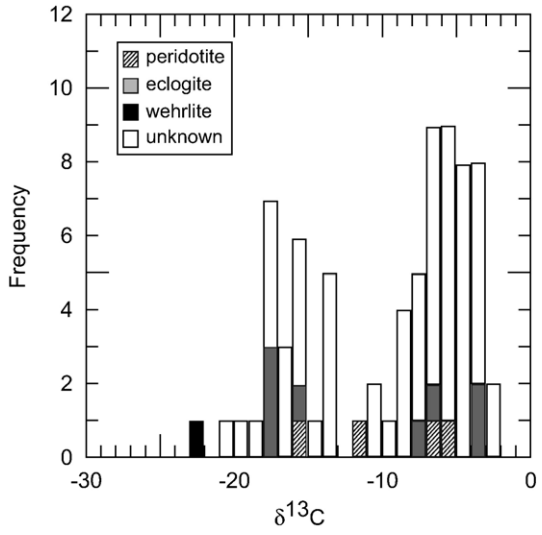

Fig. 8. Carbon isotope composition of 73 diamonds samples from pipes K11, K91 and K252. A bimodal distribution is evident with modes at −5‰ and −17‰.

7. Impurities

Nitrogen is the most abundant substitutional impurity in diamond. It enters the diamond lattice as singly substituted atoms during diamond growth, with variable amounts being incorporated. Worldwide concentrations ranging from below detection (<10 ppm) to ~ 5500 ppm have been reported (Sellschop et al., 1979). Most diamonds have nitrogen concentrations <500 ppm but many deposits exhibit broad ranges from 0 to >2500 ppm (Bibby, 1982). Buffalo Hills diamonds have nitrogen contents ranging from below detection to 3300 ppm. Variations within single diamond crystals are as high as a few hundred ppm; however, systematic variations with growth could not be assessed as nitrogen was measured on cleavage fragments after breakage. Hydrogen impurities, indicated by a narrow absorption band at 3107 cm^{-1}, were noted in 77% of the samples.

Diamonds without detectable nitrogen (i.e. ≤10 ppm) are classified as Type II. At this locality ~ 20% of the diamonds are classified as Type II (Table 1 and Supplementary Table 1). The Type II diamonds span the whole range of sizes and have a broad range of carbon isotope compositions (−16.6 to −2.5‰). Davies et al. (2004) also noted a high proportion (~ 45%) of Type II diamonds within their data set. Worldwide, Type II diamonds comprise only about 2% of the diamond population, however a small number of deposits show a higher abundance (e.g. DO27, Slave craton, (Davies et al., 1999), Akwatia, Ghana, 37%, (Stachel and Harris, 1997b); Panda, Slave craton, (Tappert et al., 2005)).

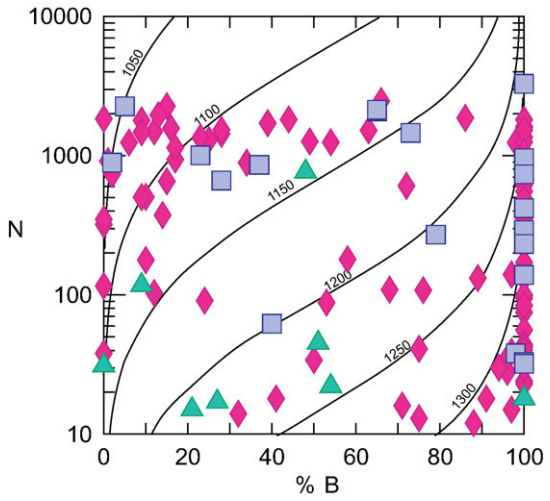

Fig. 9. Nitrogen contents and aggregation states (relative proportion of nitrogen in B-center) for diamonds from K11 (triangles), K91 (squares) and K252 (diamonds). Solid lines are isotherms (°C) for a mantle residence time of 1Ga (after Taylor et al., 1990).

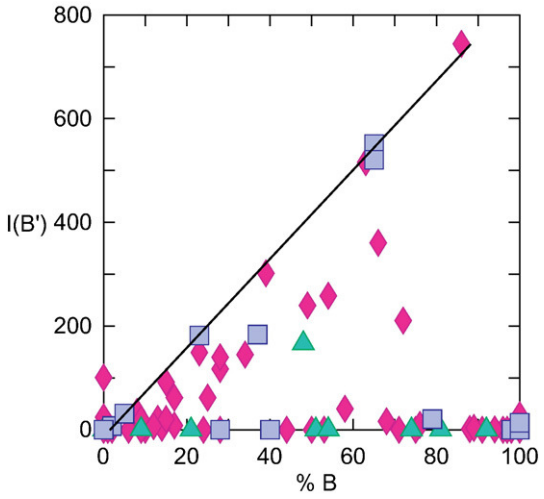

Fig. 10. The integrated absorption of the platelet peak (I(B′)) vs. the percent of nitrogen in the B-center (%B) in Type Ia diamonds (K11: triangles, K91: squares, K252: diamonds). Woods (1986) established a linear relationship between platelet intensity and nitrogen aggregation for "normal" diamonds (solid line). Most samples in this study plot below the trend line suggesting catastrophic platelet degradation, indicative of transient heating events that affected the diamonds during mantle storage (Evans et al., 1995).

Diamonds with measurable nitrogen concentrations are classified as Type I and may be further subdivided based on the aggregation state of nitrogen (Evans et al., 1981). Diamonds with nitrogen in single substitution are classified as Type Ib and are rare in nature. Diamonds with aggregated nitrogen are classified as Type Ia. Nitrogen aggregation proceeds to form pairs, classified as Type IaA and rings of four N-atoms surrounding a vacancy, classified as Type IaB (Davies, 1976; Evans et al., 1981). Type IaAB diamonds, containing nitrogen in both aggregation states, are common and often also have an absorbance peak at ~ 1370 cm^{-1} associated with platelets (Evans et al., 1981; Sobolev et al., 1968). Eighty percent of the samples in our study are Type Ia with varying stages of aggregation present at all nitrogen concentrations (Fig. 9). Aggregation in Type Ia diamonds is expressed as the relative proportion of nitrogen present in the B-center (abbreviated as %B). Type IaA (% B < 10%) comprise 10% of the population, with nitrogen concentrations between 40 and 2400 ppm. Approximately 32% of the diamonds are Type IaAB (defined as %B = 10–90%) and have nitrogen concentrations ranging from 8 ppm to 2500 ppm. About 67% of the type IaAB diamonds also show an absorbance at 1370 cm^{-1} (i.e. have a platelet component). The lack of a platelet component in 33% of the Type IaAB samples and a low platelet component in 75% of the Type IaAB samples which show platelet absorption indicates that catastrophic platelet

degradation (Woods, 1986), possibly related to transient heating events (Evans et al., 1995), occurred (Fig. 10). Type IaB (%B>90%) diamonds are the most abundant comprising 38% of the samples and show nitrogen concentrations from 6 ppm to 3300 ppm. The occurrence of diamonds with fully aggregated nitrogen (Type IaB) and very low nitrogen concentrations is highly unusual and distinct to this area.

There are major differences between the three pipes with respect to nitrogen content and distribution of aggregation states. K252 (117 diamonds) dominates the above distribution and hence the values reported above reflect mainly this pipe. K11 (21 diamonds) shows a much higher proportion of Type II diamonds, ~ 50%, and no Type IaB diamonds. K91 (23 diamonds) has only one Type II diamond and is dominated by Type IaB diamonds. The discrepancy maybe due to small sample sizes for the three pipes precluding statistically valid comparisons. K14 (29 diamonds, Davies et al., 2004) shows a distribution similar to that of K252.

8. Discussion

Studies of mantle derived xenoliths (e.g. Boyd, 1989; Griffin et al., 2003; Schulze, 1989) and inclusions in diamonds (e.g. Gurney, 1989; Harris, 1992; Meyer, 1987; Stachel et al., 2004) have shown that the subcratonic lithospheric mantle within its diamond source regions is dominated by peridotite, with only a minor eclogite component. Several lines of evidence indicate that diamonds from the Buffalo Hills kimberlites are distinct from the peridotite-dominated production of many of the classical diamond deposits (e.g. in the Kimberley area of South Africa).

8.1. Implications from carbon isotope composition

The Buffalo Hills diamonds show a high proportion of low $\delta^{13}C$ compositions associated with inclusions of eclogitic paragenesis. If this association is extended to the diamonds without inclusions for which only carbon isotope data are available it implies that the composition of the diamond-bearing mantle beneath the Buffalo Head Terrane is dominated by eclogite with only a minor peridotitic component. This places the Buffalo Hills within a small group of deposits worldwide that are characterized by a predominance of eclogitic diamonds including the Argyle lamproite (Jaques et al., 1989); the Orapa (Gurney et al., 1984), the Premier (Gurney et al., 1985), and the Jwaneng kimberlite pipes (Deines et al., 1997), and the Guaniamo deposits (Kaminsky et al., 2000). On the Kalahari craton a high proportion of eclogitic diamonds is characteristic of areas that were affected by Proterozoic tectonothermal events (Shirey et al., 2002). The Argyle and Guaniamo deposits are also located within cratons which experienced extensive Proterozoic tectonothermal activity (Jaques et al., 1989; Kaminsky et al., 2000). However, these areas retained an Archean subcontinental lithospheric mantle, while an Archean signature is not preserved in the Buffalo Head Terrane (Aulbach et al., 2004).

The source of isotopically light carbon for diamonds is still debated. The broad range in $\delta^{13}C$ exhibited by eclogitic diamonds encompasses the typical isotopic compositions of organic matter, $\delta^{13}C \sim -35$ to -20‰, and marine carbonates, $\delta^{13}C \sim -2$ to $+2$‰ (Kirkley et al., 1991). This has led to the suggestion that subducted oceanic crust containing organic matter and marine carbonates is involved in the formation of eclogitic diamonds. Subducting basaltic oceanic crust recrystallizes to eclogite during prograde metamorphism, the accompanying carbonaceous material would be converted to eclogitic diamond (Kirkley et al., 1991; McCandless and Gurney, 1997). Alternatively, the broad range of $\delta^{13}C$ values in eclogites could be created through fractionation processes. An unbuffered, free CO_2-fluid phase can exist in eclogite (Luth, 1993), escape of CO_2 (e.g. from an ascending carbonatite) would leave an isotopically depleted residue encompassing the observed isotopic range (Cartigny et al., 1998a). Diamonds formed from the residual carbon would encompass the range of light $\delta^{13}C$ values observed in eclogitic diamonds. In peridotite, CO_2 is buffered by the presence of olivine and orthopyroxene (Brey et al., 1983; Knoche et al., 1999; Wyllie and Huang, 1976) and hence fractionation of carbon isotopes involving an oxidized fluid phase cannot occur.

8.2. Sublithospheric diamonds

The incorporation of nitrogen into the diamond lattice is not fully understood. It has been suggested that the uptake of nitrogen is a function of the growth rate of the diamond (Boyd et al., 1994b; Cartigny et al., 2001). In this case slower growth would cause less nitrogen to be incorporated into the diamond lattice. Additionally, based on observations that diamonds of similar $\delta^{13}C$ composition and paragenetic association have varied nitrogen contents, Deines et al. (1989) suggested that local variations in nitrogen content exist in the mantle and influence nitrogen concentrations in diamond. Furthermore an association of nitrogen-free diamonds with a deep origin has been reported from various occurrences (Davies et al., 1999; Hutchison et al., 1999; Kaminsky and Khachatryan, 2001; Stachel et al., 2002). A large proportion of Type II

diamonds is a distinguishing characteristic of the Buffalo Head Terrane and may suggest that a portion of the diamonds grew under stable conditions at high temperatures (great depth).

The remaining nitrogen-bearing diamonds have variable nitrogen concentrations and aggregation states suggesting they are derived from multiple populations. The kinetics of nitrogen aggregation has been quantified experimentally and is understood to be dependent on nitrogen concentration, temperature and storage time (Evans and Harris, 1989). Plastic deformation may increase the rate of nitrogen aggregation, hence the dataset was tested for a possible correlation between nitrogen concentration, aggregation and evidence of deformation (lamination lines, color) in the diamonds. However, no correlation between nitrogen concentration/aggregation state and deformation is evident in the Buffalo Hills samples. This is important when considering the implications of Type IaB diamonds, especially those with low nitrogen concentrations. Although some of these diamonds show signs of deformation, most appear undeformed and consequently the high aggregation must be caused by a different mechanism: high time averaged mantle residence temperature. Time averaged temperatures do not distinguish between storage at constant temperature and for example, formation in a very hot environment, in which the nitrogen aggregates quickly, and subsequent storage for longer periods in a cool lithosphere. Considering Type IaB diamonds with the lowest nitrogen concentrations, under normal lithospheric conditions, at temperatures below 1250 °C, the time required to fully aggregate such low nitrogen concentrations exceeds the age of the earth. If these diamonds had formed and been stored in the lithosphere then a very high geothermal gradient below the Buffalo Head Terrane would be required. This is contrary to the "normal" geothermal gradient of ~ 38–39 mW/m^2 reported by Aulbach et al. (2004) from their xenocryst analyses. Alternatively, the diamonds could have formed and been stored under sublithospheric conditions which would produce the observed aggregation states and nitrogen contents within reasonable residence times (e.g. 1 Ga; Fig. 9).

Additional evidence for sublithospheric diamond formation beneath the Buffalo Head Terrane is derived from the presence of majoritic garnet inclusions with formation depths of ~ 300–400 km. All the majoritic inclusions are associated with Type II diamonds. This strengthens the assumption that part of the Type II diamond population could be derived from a sublithospheric source. Furthermore, Davies et al. (2004) report in a Type II diamond the recovery of a ferropericlase inclusion suggestive of diamond sources in the lower mantle.

8.3. Lithospheric diamonds

The Type IaAB diamonds are associated with both the eclogitic and peridotitic suites. The diamonds have variable aggregation states and nitrogen contents consistent with lower temperatures (Fig. 9) and thus shallower depths typical of "normal" lithospheric conditions.

The Type IaA diamonds indicate either that diamond storage occurred at even lower temperatures (shallower depths) or that there was a younger phase of diamond formation.

8.4. Diamond growth beneath the Buffalo Head Terrane

Multiple phases of diamond formation are supported by the data collected in this study. Formation under sublithospheric conditions is supported by the presence of a majorite inclusion in diamond and the high abundance of Type II and Type IaB diamonds. Davies et al. (2004) also noted the presence of majorite inclusions and proposed crystallization in the asthenosphere and exhumation by an ascending plume or mantle convection. The three majorites recovered from two diamonds by Davies et al. (2004) from K14 have Mg-numbers of 54–56, constant CaO of 11 wt.%, TiO_2 of 1.3–1.6 wt.% and Na_2O of 1.5–1.6 wt.%. Such compositions are inconsistent with precipitation from very deep seated melts, e.g. associated with an ascending plume, and suggest formation in a source of "basaltic" bulk composition. The lherzolitic majorite recovered from K11 has 6.3 wt.% Cr_2O_3, again a signature inconsistent with a high pressure origin but indicative of a source that experienced previous melt depletion at low pressure (Stachel et al., 1998 and references therein). We interpret these majorite inclusions to indicate formation over a depth range of ~ 300–400 km both in the eclogitic and peridotitic regions of a subducting oceanic slab. At the 660 km discontinuity subducting slabs may become buoyant forming, over time, large accumulations (megaliths) of relatively cool but deformed former oceanic lithosphere (Ringwood, 1991). A portion of the Type II and Type IaB diamonds may have formed under transition zone and lower mantle conditions in such a megalith. The single ferropericlase inclusion recovered by Davies et al. (2004) may reflect the lower mantle portion of this megalith.

The remaining diamonds formed under "normal" conditions in the lithospheric mantle. The large range of carbon isotopic compositions for lithospheric eclogitic

and wehrlitic diamonds may result from isotopic fractionation within a percolating C–H–O fluid/melt or may point to variable organic input. Infiltrating fluids of carbonatitic affinity could be the source of the Ca-enrichment needed to form the wehrlitic suite.

Transport of transition zone and lower mantle diamonds to the base of the lithosphere through mantle plumes, as envisaged by Davies et al. (2004), is certainly viable. Alternatively, disaggregation and melting of megaliths and the surrounding pyrolite may generate melt batches that ascend more rapidly towards the lithosphere and that may directly relate to kimberlite volcanism. A temporal link between exhumation of ultradeep diamonds and kimberlite activity is indicated by the unexsolved nature of majorite inclusions in the Buffalo Hills diamonds. Within its primary stability field diamond is not a rigid pressure vessel but deforms plastically through slip along octahedral planes (De Vries, 1975). If sub-lithospheric diamonds had resided within the lithospheric mantle for extended periods of time, majorite garnet should have converted to touching inclusion pairs of "normal" garnet and pyroxene. The observation that pyroxene exsolutions are absent suggests rapid exhumation from the transition zone and asthenosphere in a kimberlite magma (Ringwood et al., 1992) leading to Cretaceous volcanism in the Buffalo Hills.

9. Conclusions

The Buffalo Hills kimberlites intrude the Proterozoic Buffalo Head Terrane, a setting uncharacteristic for economically viable diamond occurrences. The recovered xenocryst and xenolith suites show a scarcity of typical mantle indicator minerals suggesting an atypical mantle composition (Aulbach et al., 2004; Hood and McCandless, 2004). A lack of typical inclusion minerals such as harzburgitic garnet is also observed for the diamonds. A high relative abundance of eclogitic inclusions and low $\delta^{13}C$ diamonds and the presence of a wehrlitic inclusion paragenesis point to mantle sources which are distinctly different from those of diamond occurrences worldwide. Additionally, the observation of a high abundance of Type II and Type IaB diamonds combined with the presence of majorite inclusions indicate that a portion of the diamonds are of sublithospheric origin, probably derived from an oceanic slab and resulting megalith. Combined these characteristics define a deposit which is distinctive in character from typical diamond deposits and emphasize that unconventional tectonic settings may host economically viable diamond deposits albeit with unique characteristics.

Acknowledgements

Ashton Mining Canada, Pure Gold and Encana are thanked for supplying the diamond samples. We are grateful to Sergei Matveev for his endless help on the electron microprobe. Steven Creighton is thanked for his numerous entertaining and informative discussions. A.B. is very grateful to Jeff Harris for her introduction to the world of diamonds. A.B. would like to acknowledge support from NSERC under the Post Graduate Scholarship-A (PGS-A). T.S. acknowledges funding through NSERC and the Canada Research Chairs program (CRC). This manuscript benefited from the constructive criticism of Rondi Davies and two more anonymous reviewers.

Appendix A. Supplementary data

Supplementary data associated with this article can be found, in the online version, at doi:10.1016/j.lithos.2006.07.001.

References

Aulbach, S., Griffin, W.L., O'Reilly, S.Y., McCandless, T.E., 2004. Genesis and evolution of the lithospheric mantle beneath the Buffalo Head Terrane, Alberta (Canada). Lithos 77 (1–4), 413–451.

Bibby, D.M., 1982. Impurities in natural diamond. Chemistry and Physics of Carbon 18, 1–91.

Boyd, F.R., 1989. Compositional distinction between oceanic and cratonic lithosphere. Earth and Planetary Science Letters 96 (1–2), 15–26.

Boyd, S.R., Kiflawi, I., Woods, G.S., 1994a. The relationship between infrared absorption and the A defect concentration in diamond. Philosophical Magazine B 69 (6), 1149–1153.

Boyd, S.R., Pineau, F., Javoy, M., 1994b. Modelling the growth of natural diamonds. Chemical Geology 116, 29–42.

Boyd, S.R., Kiflawi, I., Woods, G.S., 1995. Infrared absorption by the B nitrogen aggregate in diamond. Philosophical Magazine B 72 (3), 351–361.

Brey, G., Brice, W.R., Ellis, D.J., Green, D.H., Harris, K.L., Ryabchikov, I.D., 1983. Pyroxene-carbonate reactions in the upper mantle. Earth and Planetary Science Letters 62, 63–74.

Carlson, S.M., Hillier, W.D., Hood, C.T., Pryde, R.P., Skelton, D.N., 1999. The Buffalo Hills kimberlites: a newly discovered diamondiferous kimberlite province in North–central Alberta, Canada. In: Gurney, J.J., Gurney, J.L., Pascoe, M.D., Richardson, S.H. (Eds.), The J.B. Dawson Volume, Proceedings of the VIIth International Kimberlite Conference. Red Roof Design, Cape Town, SA, pp. 109–116.

Cartigny, P., Harris, J.W., Javoy, M., 1998a. Eclogitic diamond formation at Jwaneng: no room for a recycled component. Science 280 (5368), 1421–1424.

Cartigny, P., Harris, J.W., Phillips, D., Girard, M., Javoy, M., 1998b. Subduction-related diamonds? The evidence for a mantle-derived origin from coupled $\delta^{13}C$–$\delta^{13}N$ determinations. Chemical Geology 147 (1–2), 147–159.

Cartigny, P., Harris, J.W., Javoy, M., 2001. Diamond genesis, mantle fractionations and mantle nitrogen content: a study of $\delta^{13}C$–N concentrations in diamonds. Earth and Planetary Science Letters 185 (1–2), 85–98.

Davies, G., 1976. The A nitrogen aggregate in diamond — its symmetry and possible structure. Journal of Physics C: Solid State Physics 9, L537–L542.

Davies, R.M., Griffin, W.L., Pearson, N.J., Andrew, A.S., Doyle, B.J., O'Reilly, S.Y., 1999. Diamonds from the deep: pipe DO-27, Slave Craton, Canada. In: Gurney, J.J., Gurney, J.L., Pascoe, M.D., Richardson, S.H. (Eds.), The J.B. Dawson Volume, Proceedings of the VIIth International Kimberlite Conference. Red Roof Design, Cape Town, pp. 148–155.

Davies, R.M., Griffin, W.L., O'Reilly, S.Y., McCandless, T.E., 2004. Inclusions in diamonds from the K14 and K10 kimberlites, Buffalo Hills, Alberta, Canada: diamond growth in a plume? Lithos 77 (1–4), 99–111.

Deines, P., Harris, J.W., Spear, P.M., Gurney, J.J., 1989. Nitrogen and ^{13}C content of Finsch and Premier diamonds and their implications. Geochimica et Cosmochimica Acta 53 (6), 1367–1378.

Deines, P., Harris, J.W., Gurney, J.J., 1997. Carbon isotope ratios, nitrogen content and aggregation state, and inclusion chemistry of diamonds from Jwaneng, Botswana. Geochimica et Cosmochimica Acta 61 (18), 3993–4005.

De Vries, R.C., 1975. Plastic deformation and "work-hardening" of diamond. Materials Research Bulletin 10, 1193–1200.

Eccles, D., Pana, D., Paulen, R., Olson, R., Magee, D., 2003. Discovery and geological setting of the northern Alberta kimberlite province. In: Kjarsgaard, B. (Ed.), 8th International Kimberlite Conference, Slave Province and Northern Alberta Field Trip Guidebook, pp. 1–10.

Evans, T., Harris, J.W., 1989. Nitrogen aggregation, inclusion equilibration temperatures and the age of diamonds. In: Ross, J., et al. (Ed.), Kimberlites and Related Rocks. Geological Society of Australia, Special Publication 14, vol. 2. Blackwell, Carlton, pp. 1001–1006.

Evans, T., Kiflawi, I., Luyten, W., Vantendeloo, G., Woods, G.S., 1995. Conversion of platelets into dislocation loops and voidite formation in Type IaB diamonds. Proceedings of the Royal Society of London Series A—Mathematical and Physical Sciences 449 (1936), 295–313.

Evans, T., Qi, Z., Maguire, J., 1981. The stages of nitrogen aggregation in diamond. Journal of Physics C: Solid State Physics 14 (12), L379–L384.

Griffin, W.L., O'Reilly, S.Y., Ryan, C.G., 1999. The composition and origin of subcontinental lithospheric mantle. In: Fei, Y., Bertka, C.M., Mysen, B.O. (Eds.), Mantle Petrology: Field Observations and High Pressure Experimentation: A tribute to Francis R. (Joe) Boyd. Special Publication. The Geochemical Society, Houston, pp. 13–45.

Griffin, W.L., O'Reilly, S.Y., Natapov, L.M., Ryan, C.G., 2003. The evolution of lithospheric mantle beneath the Kalahari Craton and its margins. Lithos 71 (2–4), 215–241.

Gurney, J.J., 1989. Diamonds. In: Ross, J., et al. (Ed.), Kimberlites and Related Rocks. Geological Society of Australia, Special Publication 14, vol. 2. Blackwell, Carlton, pp. 1001–1006.

Gurney, J.J., Harris, J.W., Rickard, R.S., 1984. Silicate and oxide inclusions in diamonds from the Orapa Mine, Botswana. In: Kornprobst, J. (Ed.), Kimberlites II: The Mantle and Crust–Mantle Relationships. Elsevier, Amsterdam, pp. 3–9.

Gurney, J.J., Harris, J.W., Rickard, R.S., Moore, R.O., 1985. Premier mine diamond inclusions. Transactions of the Geological Society of South Africa 88, 301–310.

Harris, J.W., 1987. Recent physical, chemical, and isotopic research of diamond. In: Nixon, P.H. (Ed.), Mantle Xenoliths. John Wiley and Sons Ltd., Chichester, pp. 477–500.

Harris, J.W., 1992. Diamond geology. In: Field, J.E. (Ed.), The Properties of Natural and Synthetic Diamond. Academic Press, London, pp. 345–393.

Hood, C.T.S., McCandless, T.E., 2004. Systematic variations in xenocryst mineral composition at the province scale, Buffalo Hills kimberlites, Alberta, Canada. Lithos 77 (1–4), 733–747.

Hutchison, M.T., Cartigny, P., Harris, J.W., 1999. Carbon and nitrogen compositions and physical characteristics of transition zone and lower mantle diamonds from Sao Luiz, Brazil. In: Gurney, J.J., Gurney, J.L., Pascoe, M.D., Richardson, S.H. (Eds.), The J.B. Dawson Volume, Proceedings of the VIIth International Kimberlite Conference. Red Roof Design, Cape Town, pp. 372–382.

Irifune, T., 1987. An experimental investigation of the pyroxene–garnet transformation in a pyrolite composition and its bearing on the constitution of the mantle. Physics of the Earth and Planetary Interiors 45 (4), 324–336.

Janse, A.J.A., 1994. Is Clifford's rule still valid? Affirmative examples from around the world. In: Meyer, H.O.A., Leonardos, O.H. (Eds.), Diamonds: Characterization, Genesis and Exploration. CPRM — Special Publication Jan/94, Brasilia, pp. 215–235.

Jaques, A.L., Hall, A.E., Sheraton, J.W., Smith, C.B., Sun, S.-S., Drew, R.M., Foudoulis, C., Ellingsen, K., 1989. Composition of crystalline inclusions and C-isotopic composition of Argyle and Ellendale diamonds. In: Ross, J., et al. (Ed.), Kimberlites and Related Rocks. Geological Society of Australia, Special Publication 14, vol. 2. Blackwell, Carlton, pp. 966–989.

Kaminsky, F.V., Khachatryan, G.K., 2001. Characteristics of nitrogen and other impurities in diamond, as revealed by infrared absorption data. Canadian Mineralogist 39, 1733–1745.

Kaminsky, F.V., Zakharchenko, O.D., Griffin, W.L., Channer, D.M.D., Khachatryan-Blinova, G.K., 2000. Diamond from the Guaniamo area, Venezuela. Canadian Mineralogist 38, 1347–1370.

Kirkley, M.B., Gurney, J.J., Otter, M.L., Hill, S.J., Daniels, L.R., 1991. The application of C isotope measurements to the identification of the sources of C in diamonds: a review. Applied Geochemistry 6 (5), 477–494.

Knoche, R., Sweeney, R.J., Luth, R.W., 1999. Carbonation and decarbonation of eclogites: the role of garnet. Contributions to Mineralogy and Petrology 135 (4), 332–339.

Köhler, T., Brey, G.P., 1990. Calcium exchange between olivine and clinopyroxene calibrated as geothermobarometer for natural peridotites from 2 to 60 kb with applications. Geochimica et Cosmochimica Acta 54, 2375–2388.

Kopylova, M.G., Russell, J.K., Stanley, C., Cookenboo, H., 2000. Garnet from Cr- and Ca-saturated mantle: implications for diamond exploration. Journal of Geochemical Exploration 68 (3), 183–199.

Luth, R.W., 1993. Diamonds, eclogites, and the oxidation state of the Earth's mantle. Science 261 (5117), 66–68.

McCandless, T.E., Gurney, J.J., 1997. Diamond eclogites: comparison with carbonaceous chondrites, carbonaceous shales, and microbial carbon-enriched MORB. Geologiya i Geofizika 38 (2), 371–381.

Meyer, H.O.A., 1987. Inclusions in diamond. In: Nixon, P.H. (Ed.), Mantle Xenoliths. John Wiley and Sons Ltd., Chichester, pp. 501–522.

Mossop, G., Shetsen, I. (compilers), 1994. Geological Atlas of the Western Canada Sedimentary Basin. Canadian Society of Petroleum Geologists and Alberta Research Council, Calgary, AB. 510 pp.

Orlov, Y., 1973. The Mineralogy of Diamond. John Wiley and Sons. 264 pp.

Ringwood, A.E., 1991. Phase transformations and their bearing on the constitution and dynamics of the mantle. Geochimica et Cosmochimica Acta 55 (8), 2083–2110.

Ringwood, A.E., Kesson, S.E., Hibberson, W., Ware, N., 1992. Origin of kimberlites and related magmas. Earth and Planetary Science Letters 113 (4), 521–538.

Robinson, D.N., 1979. Surface textures and other features of diamonds. Unpublished PhD thesis. University of Cape Town. 221 pp.

Robinson, D.N., Scott, J.A., van Niekerk, A., Anderson, V.G., 1989. The sequence of events reflected in the diamonds of some southern African kimberlites. In: Ross, J., et al. (Ed.), Kimberlites and Related Rocks. Geological Society of Australia Special Publication 14. Blackwell, Carlton, pp. 990–1000.

Schulze, D.J., 1989. Constraints on the abundance of eclogite in the upper mantle. Journal of Geophysical Research: Solid Earth and Planets 94 (B4), 4205–4212.

Sellschop, J.P.F., Madiba, C.C.P., Annegarn, H.J., Shongwe, S., 1979. Volatile light elements in diamond. Diamond Research. Industrial Diamond Information Bureau, London, United Kingdom, pp. 24–30.

Shirey, S.B., Harris, J.W., Richardson, S.H., Fouch, M.J., James, D.E., Cartigny, P., Deines, P., Viljoen, F., 2002. Diamond genesis, seismic structure, and evolution of the Kaapvaal–Zimbabwe craton. Science 297 (5587), 1683–1686.

Sobolev, E.V., Lisoivan, V.I., Lenskaya, S.V., 1968. The relation between the "spike" extra reflections in the Laue patterns of natural diamonds and their optical properties. Soviet Physics–Crystallography 12, 665–668.

Sobolev, N.V., Lavrent'ev, Y.G., Pokhilenko, N.P., Usova, L.V., 1973. Chrome-rich garnets from the kimberlites of Yakutia and their paragenesis. Contributions to Mineralogy and Petrology 40 (1), 39–52.

Sobolev, N.V., Pokhilenko, N.P., Efimova, E.S., 1984. Diamond bearing peridotite xenoliths in kimberlites and the problem of the origin of diamonds. Geologiya i Geofizika 25 (12), 62–76.

Sobolev, N.V., Logvinova, A.M., Zedgenizov, D.A., Seryotkin, Y.V., Yefimova, E.S., Floss, C., Taylor, L.A., 2004. Mineral inclusions in microdiamonds and macrodiamonds from kimberlites of Yakutia: a comparative study. Lithos 77 (1–4), 225–242.

Stachel, T., Harris, J.W., 1997a. Syngenetic inclusions in diamond from the Birim field (Ghana) — a deep peridotitic profile with a history of depletion and re-enrichment. Contributions to Mineralogy and Petrology 127 (4), 336–352.

Stachel, T., Harris, J.W., 1997b. Diamond precipitation and mantle metasomatism — evidence from the trace element chemistry of silicate inclusions in diamonds from Akwatia, Ghana. Contributions to Mineralogy and Petrology 129 (2–3), 143–154.

Stachel, T., Harris, J.W., Brey, G.P., 1998. Rare and unusual mineral inclusions in diamonds from Mwadui, Tanzania. Contributions to Mineralogy and Petrology 132 (1), 34–47.

Stachel, T., Brey, G.P., Harris, J.W., 2000. Kankan diamonds (Guinea) I: from the lithosphere down to the transition zone. Contributions to Mineralogy and Petrology 140, 1–15.

Stachel, T., Harris, J.W., Aulbach, S., Deines, P., 2002. Kankan diamonds (Guinea) III: $\delta^{13}C$ and nitrogen characteristics of deep diamonds. Contributions to Mineralogy and Petrology 142 (4), 465–475.

Stachel, T., Aulbach, S., Brey, G., Harris, J.W., Leost, I., Tappert, R., Viljoen, K.S., 2004. The trace element composition of silicate inclusions in diamonds: a review. Lithos 77, 1–19.

Tappert, R., Stachel, T., Harris, J.W., Shimizu, N., Brey, G., 2005. Mineral inclusions in diamonds from the Panda kimberlite, Salve Province, Canada. European Journal of Mineralogy 17, 423–440.

Taylor, W.R., Jaques, A.L., Ridd, M., 1990. Nitrogen-defect aggregation characteristics of some Australasian diamonds: time–temperature constraints on the source regions of pipe and alluvial diamonds. American Mineralogist 75 (11–12), 1290–1310.

Theriault, R.J., Ross, G.M., 1991. Nd isotopic evidence for crustal recycling in the ca. 2.0 Ga subsurface of Western Canada. Canadian Journal of Earth Sciences 28 (8), 1140–1147.

Villeneuve, M.E., Ross, G.M., Theriault, R.J., Parrish, R.R., Broome, J., 1993. Tectonic subdivision and U–Pb geochronolgy of the crystalline basement of the Alberta basin, Western Canada. Geological Survey of Canada, Bulletin 447. 85 p.

Woods, G.S., 1986. Platelets and the Infrared-absorption of Type-Ia diamonds. Proceedings of the Royal Society of London Series A 407 (1832), 219–238.

Wyllie, P.J., Huang, W.L., 1976. Carbonation and melting reactions in the system $CaO–MgO–SiO_2–CO_2$ at mantle pressures with geophysical and petrological applications. Contributions to Mineralogy and Petrology 54, 79–107.